Journal of Power Sources 196 (2011) 7500–7504

Contents lists available at ScienceDirect

Journal of Power Sources

journal homepage: www.elsevier.com/locate/jpowsour

Short communication

Novel $BaCe_{0.7}In_{0.2}Yb_{0.1}O_{3-\delta}$ proton conductor as electrolyte for intermediate temperature solid oxide fuel cells

Fei Zhao, Siwei Wang, Latoya Dixon, Fanglin Chen*

Department of Mechanical Engineering, University of South Carolina, Columbia, SC 29208, USA

ARTICLE INFO

Article history:
Received 4 February 2011
Received in revised form 15 April 2011
Accepted 15 April 2011
Available online 22 April 2011

Keywords:
Proton conductor
Conductivity
Performance
Durability

ABSTRACT

Novel proton conductor $BaCe_{0.7}In_{0.2}Yb_{0.1}O_{3-\delta}$ (BCIYb) has been successfully synthesized by a modified Pechini method and characterized as electrolyte for intermediate temperature solid oxide fuel cells. Acceptable tolerance to wet CO_2 environment was found during chemical stability tests. No interaction between the BCIYb electrolyte and $La_{0.6}Sr_{0.4}Co_{0.2}Fe_{0.8}O_{3-\delta}$ (LSCF) cathode was observed during the cathode fabrication process. Further, no detectable impurity phase was found when the BCIYb–LSCF mixed powders were calcined at 700 °C for 50 h. BCIYb dense samples sintered at 1450 °C for 5 h showed acceptable conductivities of 7.2×10^{-3}, 8×10^{-3}, 4.5×10^{-3} and 3.1×10^{-3} S cm^{-1} at 800 °C in dry air, wet air, wet H_2 and wet N_2, respectively. The maximum cell power outputs of single cells with the configuration of Ni–$BaZr_{0.1}Ce_{0.7}Y_{0.2}O_{3-\delta}$ (BZCY)|BCIYb|BZCY–LSCF were 0.15, 0.218 and 0.28 W cm^{-2} at 600, 650 and 700 °C, respectively. No cell degradation was observed for cells operated at a constant voltage of 0.7 V in the 25 h short-term durability test.

1. Introduction

Development of new materials for solid oxide fuel cells (SOFCs) is crucial to effectively reduce the cost of SOFCs operated at intermediate temperatures [1]. Proton conductors are promising electrolytes for intermediate temperature SOFCs and have received increasing attentions due to their low activation energy for proton transport [2–5]. Solid state proton conductors can be used in a wide variety of applications such as proton conducting SOFCs, solid state electrolyzer cells, high temperature hydrogen sensors, hydrogen separation membranes, and hydrogen pumps [6–8]. Among the different types of solid state proton conductors studied for elevated temperature operations, perovskite-type oxides based on cerate such as $BaCeO_3$ and $SrCeO_3$ and zirconate such as $BaZrO_3$ exhibit high protonic or mixed ionic conductivity in environments containing hydrogen and/or water vapor at elevated temperatures [9,10]. The proton conduction originates from the protonic defects in the ABO_3 perovskites due to dissociative adsorption of water or hydrogen in the presence of oxygen vacancies. The oxygen vacancies thereafter react with oxygen to produce electron holes in an oxygen rich environment, or react with water to produce protons in a water rich environment [11]. The defect chemistry reactions are described as

$$\frac{1}{2}O_2\ (g) + V^{\bullet\bullet}_O = O^x_O + 2h^{\bullet} \quad (1)$$

$$H_2O\,(g) + V^{\bullet\bullet}_O + O^x_O = 2OH^{\bullet}_O \quad (2)$$

The dissolution of water vapor takes place at the oxygen vacancy sites and forms mobile protons in the oxides, hopping on the oxygen sites by forming $OH^{\bullet}_O$. The mechanism of proton migration was proposed by Iwahara [12] and further analyzed by Kreuer [13]. Since the protonic defect is formed in the oxides, the oxygen vacancy concentration plays an important role in proton conduction.

In the past three decades, researchers have discovered several perovskite-type oxides exhibiting high proton conductivity at elevated temperatures. Among them, doped barium cerates, $BaCe_{1-x}A_xO_{3-\delta}$ (A = Nd^{3+}, Sm^{3+}, Gd^{3+}, Eu^{3+}, Yb^{3+}, Y^{3+}, and In^{3+}), have exhibited particularly high proton conductivity [14–20]. Unfortunately, doped barium cerates have poor chemical stability at elevated temperatures in the presence of CO_2 and water vapor, raising serious concerns for the durability of SOFCs using such materials as electrolytes [21]. One effective approach to improve the chemical stability of barium cerate-based proton conductor is to form a solid solution with barium zirconate. Although zirconate-based proton conductors have much lower conductivity, they are relatively more stable than the barium cerate-based proton conductor at elevated temperatures in CO_2 and/or in humid atmospheres. Since $BaCeO_3$ and $BaZrO_3$ can easily form a solid solution across their entire composition range, replacing a fraction of Ce in $BaCeO_3$ with Zr can achieve a solid solution of cerate and zirconate with

* Corresponding author. Tel.: +1 803 777 4875; fax: +1 803 777 0106.
E-mail address: chenfa@cec.sc.edu (F. Chen).

0378-7753/$ – see front matter © 2011 Elsevier B.V. All rights reserved.
doi:10.1016/j.jpowsour.2011.04.036

both good protonic conductivity and chemical stability. For example, Osman reported that introduction of 20 mol% Zr improved the chemical stability of $BaCe_{0.95}Yb_{0.05}O_{2.975}$ sample in atmosphere containing CO_2 at 600 °C [22]. It has also been reported that $BaZr_{0.1}Ce_{0.7}Y_{0.2}O_{3-\delta}$ (BZCY) exhibits not only adequate proton conductivity but also sufficient chemical and thermal stability over a wide range of conditions relevant to SOFC operations [23,24].

Another strategy to improve the chemical stability of barium cerate-based proton conductor is through co-doping B-sites with two or more aliovalent ions with lower valence. Such strategy has been successfully applied on doped $BaCeO_3$ with M (M = Ta, Ti, Nb, and Sn) and Y as the co-dopants and proved to maintain both high conductivity and good stability [25–28]. Consequently, the co-doping strategy has been explored in this study for $BaCeO_3$ co-doped with In and Yb in order to enhance the chemical stability without remarkably sacrificing the proton conductivity. In-doped barium cerate has recently been reported to maintain good stability at elevated temperatures in CO_2 and water vapor containing environments [29,30]. However, the electrical conductivity of In-doped $BaCeO_3$ proton conductors is still relatively low [31,32]. On the other hand, due to the multivalent oxidation state of ytterbium, low third ionization potential, and comparable ionic radius with cerium, high conductivity has been reported for $SrCeO_3$ and $BaCeO_3$ doped with Yb [11,33]. $BaCe_{0.9}Yb_{0.1}O_{3-\delta}$ has been shown to possess the highest conductivity among doped barium cerates both in dry and wet oxygen atmospheres [33].

In this study, we report a novel proton conductor, $BaCe_{0.7}In_{0.2}Yb_{0.1}O_{3-\delta}$ (BCIYb), which has a similar optimized composition to our previous study [29]. The BCIYb powder was synthesized by a modified Pechini method and the cell performances were characterized with humidified hydrogen as fuel and ambient air as oxidant. Chemical stability of BCIYb proton conductor and short-term durability of single cells using BCIYb as electrolyte were also investigated.

2. Experimental

2.1. Sample synthesis and fabrication

Powder samples of doped barium cerates having the nominal composition of $BaCe_{0.7}In_{0.2}Yb_{0.1}O_{3-\delta}$ (BCIYb) and $BaZr_{0.1}Ce_{0.7}Y_{0.2}O_{3-\delta}$ (BZCY) were synthesized by a modified citrate–nitrate combustion process as reported previously [29]. BCIYb and BZCY powders were finally calcined at 1100 °C for 6 h to form pure single phase. BZCY was used as the proton-conducting component in the composite electrodes for single cells using BCIYb as electrolyte. The as-prepared BCIYb powder was dry-pressed at 300 MPa, followed by sintering at 1450 °C for 5 h in air to obtain pellets with relative density higher than 95% for conductivity measurement and chemical stability tests.

Anode supported cells based on BCIYb electrolyte were prepared using a co-pressing and co-sintering method [34]. Anode powder consisted of 60 wt.% NiO (J.T. Baker) and 40 wt.% BZCY was firstly dry-pressed into a substrate. BCIYb powder was then added onto the substrate and co-pressed at 300 MPa to form a bi-layer, followed by co-sintering at 1450 °C for 5 h to form a half cell. The thickness for the sintered BCIYb electrolyte membrane was ~30 μm. A cathode ink consisting of BZCY-$La_{0.6}Sr_{0.4}Co_{0.2}Fe_{0.8}O_{3-\delta}$ (LSCF, Fuel Cell Materials) and a commercial binder (V-006, Heraeus) prepared by ball-milling for 24 h was applied by a screen-printing technique onto the surface of the BCIYb electrolyte membrane, followed by sintering at 1100 °C for 2 h to obtain a single cell. The thickness of the cathode was approximately 40 μm and the effective area of the cathode was 0.33 cm^2.

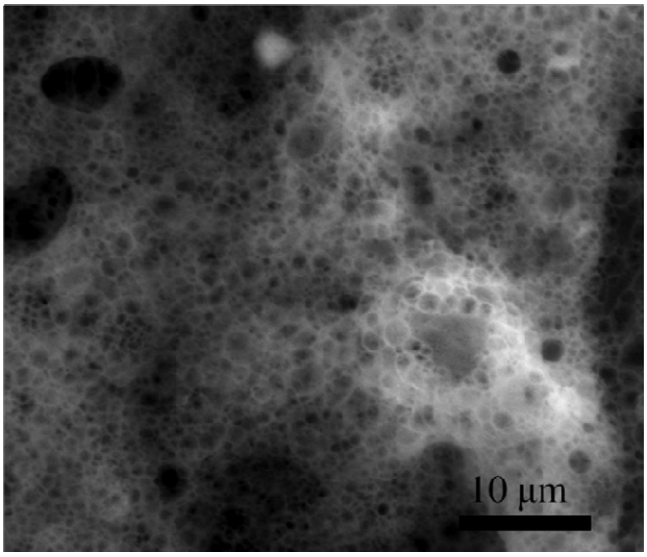

Fig. 1. SEM micrograph of BCIYb powder calcined at 1100 °C for 6 h.

2.2. Sample characterization

Pt paste was applied on both sides of the sintered BCIYb pellets and calcined at 950 °C for 0.5 h in air to form porous Pt current collector for conductivity measurement. Single cells were sealed in alumina tubes for cell performance evaluation. The crystalline structure of the sintered sample was measured using a X-ray powder diffractometer (Mini X-ray diffractometer with graphite-monochromatized Cu Kα radiation (λ = 1.5418 Å)), employing a scanning rate of 10° min^{-1} in the 2θ range of 20–80°. Microstructures of the cells were characterized using a FEI Quanta (XL 30 model) scanning electron microscope (SEM). Impedance spectra were measured on the single cells under open circuit condition, with a frequency range from 0.01 Hz to 1 MHz and a 10 mV ac perturbation, using a Versa STAT3-400 electrochemical station. The single cell performance based on the *I–V* curve was measured in the galvanostatic mode. The short-term durability of the cell was obtained in the potentiostatic mode at a constant cell voltage output of 0.7 V.

3. Results and discussion

3.1. Morphology of powder

BCIYb powder calcined at 1100 °C for 6 h in air has a foam-like morphology with plenty of voids distributed inside a porous structure as revealed from SEM analysis shown in Fig. 1. Such loose powders having very low filled density and high specific surface area are particularly suitable for fabricating thin film using a dry-pressing method.

3.2. Chemical stability

Phase formation and chemical reaction of BCIYb samples were investigated using power XRD study with results shown in Fig. 2. Since In^{3+} (0.8 Å) and Yb^{3+} (0.868 Å) have similar ionic radii to that of Ce^{4+} (0.87 Å), a solid solution is expected to form by doping In and Yb in Ce sites. Single phase perovskite structure was confirmed by XRD analysis for the BCIYb pellet sample sintered at 1450 °C for 5 h in air as shown in Fig. 2(a). When the sample was exposed to environmental air at room temperature for 2 months, no impurity peaks were found as shown in Fig. 2(b).

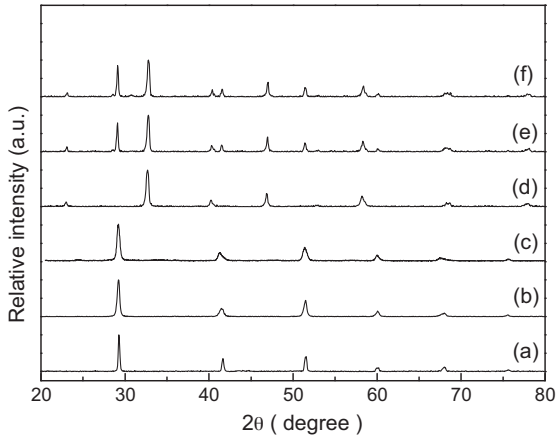

Fig. 2. X-ray diffraction patterns for (a) BCIYb pellet sample sintered at 1450 °C for 5 h in air, (b) BCIYb sample after exposure to environmental air at room temperature for 2 months, (c) BCIYb sample after exposure to wet CO_2 (3% H_2O, 3% CO_2 and air as the balance gas) at 700 °C for 24 h, (d) commercial LSCF, (e) BCIYb–LSCF cathode calcined at 1100 °C for 2 h in air, and (f) BCIYb–LSCF cathode sintered at 700 °C for 50 h in air.

Table 1
Comparison of total conductivity for doped $BaCeO_3$ in wet H_2.

Sample	Total conductivity (S cm^{-1})	
	600 °C	800 °C
$BaCe_{0.9}In_{0.1}O_{3-\delta}$ [32]	1.8×10^{-3}	3.4×10^{-3}
$BaCe_{0.9}Yb_{0.1}O_{3-\delta}$ [32]	1.5×10^{-2}	3.4×10^{-2}
$BaCe_{0.7}In_{0.2}Yb_{0.1}O_{3-\delta}$ (this work)	2.7×10^{-3}	4.5×10^{-3}
$BaCe_{0.7}In_{0.2}Y_{0.1}O_{3-\delta}$ [29]	2.6×10^{-3}	4.1×10^{-3}
$BaZr_{0.1}Ce_{0.8}Y_{0.1}O_{3-\delta}$ [41]	1×10^{-2}	1.5×10^{-2}

For the Yb-doped $BaCeO_3$ sample, XRD diffraction peaks related to $BaCeO_3$ and CeO_2 were reported by Osman et al. after the sintered sample was exposed to CO_2-containing atmosphere [35]. To investigate its tolerance to wet CO_2, the sintered BCIYb sample was heat-treated at 700 °C for 24 h by introducing a mixed gas consisting 3% H_2O, 3% CO_2 and air (balance gas). No impurity XRD diffraction peaks were detectable, as shown in Fig. 2(c), indicating that BCIYb has satisfactory tolerance to wet CO_2. The stability of Yb-doped $BaCeO_3$ is thus significantly improved by Indium co-doping, consistent with the results of In-doped $BaCeO_3$ proton-conducting materials showing good chemical stability [29]. The chemical compatibility between BCIYb power and commercial LSCF powder has also been investigated in this work. Compared Fig. 2(e) with Fig. 2(a) and (d), no impurity was observed for BCIYb–LSCF cathode calcined at 1100 °C for 2 h during the cathode fabrication process. Further, after firing the mixed powders of BCIYb and LSCF at 700 °C for 50 h in air, no apparent secondary peaks have been observed, indicating that BCIYb electrolyte and LSCF cathode material are chemically compatible.

3.3. Electrical conductivity characterization

Shown in Fig. 3 are the conductivities of the BCIYb sample measured in different atmospheres in the temperature range of 500–800 °C. Among all the examined atmospheres, BCIYb shows the highest conductivity of 8×10^{-3} S cm^{-1} at 800 °C in wet air, followed by 7×10^{-3}, 4.5×10^{-3} and 3×10^{-3} S cm^{-1} in dry air, wet hydrogen and wet nitrogen, respectively. The conductivities of BCIYb are a little bit higher than those of $BaCe_{0.7}In_{0.2}Y_{0.1}O_{3-\delta}$, which are 7×10^{-3} and 4×10^{-3} S cm^{-1} at 800 °C in wet air and wet hydrogen, respectively [29]. As shown in Table 1, the conductivity of BCIYb falls between $BaCe_{0.9}In_{0.1}O_{3-\delta}$ and $BaCe_{0.9}Yb_{0.1}O_{3-\delta}$, which are 3.4×10^{-3} and 3.4×10^{-2} S cm^{-1} at 800 °C in wet hydrogen as reported by Matsumoto et al. [32]. According to the slope of the Arrhenius plots shown in Fig. 3, the activation energies for total conductivity of the BCIYb sample were 0.4, 0.47 and 0.57 eV in wet N_2, wet air and dry air, respectively. However, slope change in wet H_2 was found in Fig. 3, showing an activation energy of 0.63 eV at temperatures below 600 °C and 0.25 eV above 600 °C, which could be related to a change of effective charge carriers' concentration [36,37].

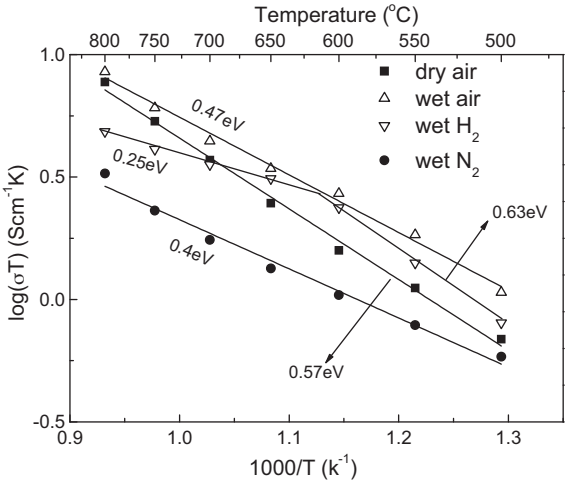

Fig. 3. Arrhenius plot of conductivity of BCIYb in different atmospheres in the temperature range of 500–800 °C.

3.4. Cell performance

To evaluate the performance of solid oxide fuel cells with BCIYb as electrolyte, the *V–I* curves and power outputs of the cells were investigated from 600 °C to 700 °C with humidified hydrogen (3 vol% H_2O) as fuel and ambient air as oxidant. As shown in Fig. 4(a), the open circuit voltages (OCVs) are 0.984, 0.981 and 0.963 V at 600, 650 and 700 °C, respectively. Maximum cell power outputs of 0.15, 0.213 and 0.28 W cm^{-2} were obtained for BCIYb-based cell at 600, 650 and 700 °C, respectively. The fuel utilization was 4.1% at 600 °C at the maximum cell power output, comparable to the testing conditions from the others [38]. Impedance spectra of the cell measured at 600, 650 and 700 °C under open circuit conditions are shown in Fig. 4(b). In the impedance spectra, the intercept with the real axis at high frequency represents the ohmic resistance of the cell, which is usually taken as the overall electrolyte resistance and contact resistance of the cell. As shown in Fig. 4(b), the ohmic resistance values of single cells using BCIYb electrolyte are 0.841, 0.745 and 0.654 Ω cm^2 at 600, 650 and 700 °C, respectively. The relatively low ohmic resistance resulted in higher cell performance compared to that of cells based on $BaCe_{0.7}In_{0.2}Y_{0.1}O_{3-\delta}$ electrolyte, which showed lower maximum power outputs of 0.114, 0.204 and 0.269 W cm^{-2} at 600, 650 and 700 °C, respectively [39]. At the same time, the polarization resistance determined by the intercept of high and low-frequency impedance curves increased with decreasing cell operating temperatures. Substantial increase in the polarization resistance was observed in low-frequency range, indicating that slow oxygen diffusion and oxygen reduction might occur in the cathode at 600 °C [40].

3.5. Short-term durability

To evaluate the durability of the cells with BCIYb as electrolyte, the cell performance as a function of time was evaluated under a constant cell voltage output of 0.7 V at 600 °C, as shown in Fig. 5.

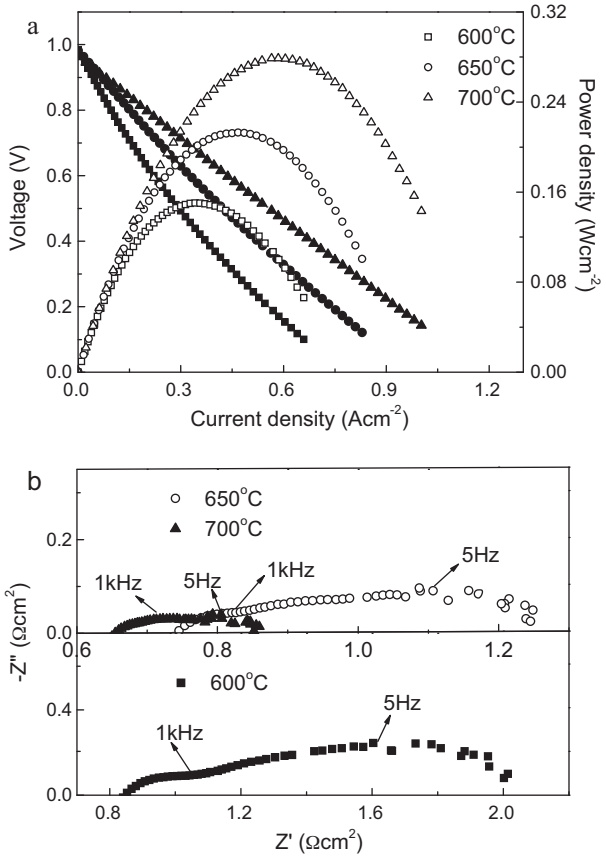

Fig. 4. Performance of the Ni–BZCY|BCIYb|LSCF–BZCY single cell. (a) Cell voltage and power density as a function of current density, (b) impedance spectra at different temperatures measured under open-circuit conditions.

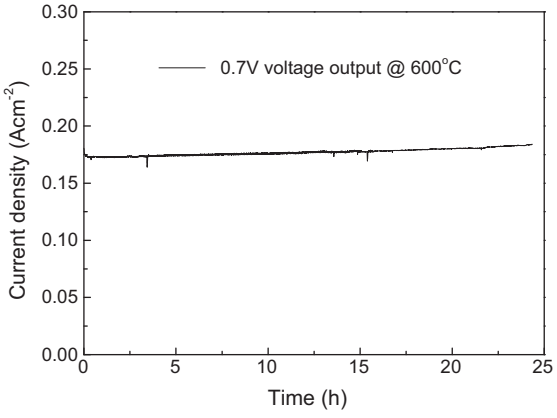

Fig. 5. Short-term durability of cell with BCIYb as electrolyte.

The current density was relatively stable and there was no obvious degradation in cell performance during the 25-h durability test for cells based on BCIYb electrolyte. Cross-section structural analysis was carried out on the single cell after the short-term performance test, and it was noticed that the anode was well bounded to the electrolyte membrane and there were no cracks in the dense electrolyte membrane as shown in Fig. 6. The short-term durability results also indicated that the BCIYb electrolyte material itself possessed sufficient chemical stability against H_2O, consistent to its good tolerance to wet CO_2-containing environment observed in the chemical stability study. Accordingly, although the conductivity for BCIYb electrolyte is not as high as that of BZCY as shown

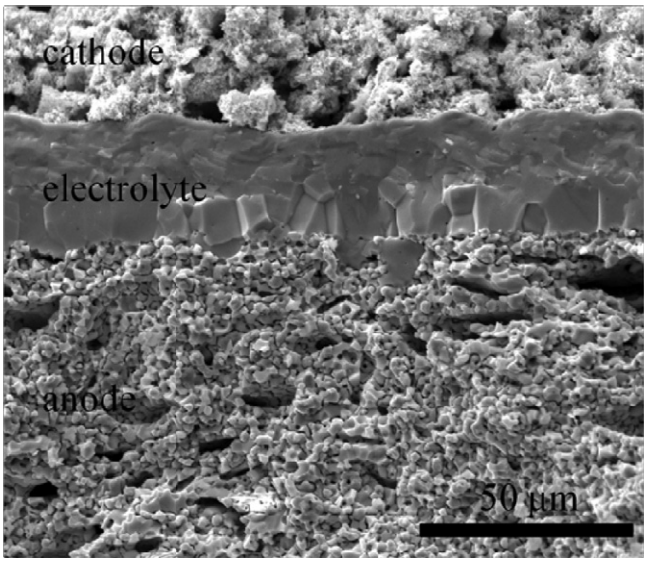

Fig. 6. SEM image of post-tested BCIYb cell.

in Table 1 [41], the durability under cell operating conditions is acceptable.

4. Conclusions

Proton conductor $BaCe_{0.7}In_{0.2}Yb_{0.1}O_{3-\delta}$ (BCIYb) was investigated as electrolyte for intermediate temperature solid oxide fuel cells. Acceptable tolerance to wet CO_2 environment and no detectable chemical reactivity between BCIYb and LSCF were found during the chemical stability tests. BCIYb dense samples sintered at 1450 °C for 5 h showed conductivities of 7.2×10^{-3}, 8×10^{-3}, 4.5×10^{-3} and 3.1×10^{-3} S cm^{-1} at 800 °C in dry air, wet air, wet H_2 and wet N_2, respectively. The single cell with BCIYb electrolyte showed maximum power outputs of 0.15, 0.218 and 0.28 W cm^{-2} at 600, 650 and 700 °C, respectively. Furthermore, no obvious cell degradation was observed during the 25-h durability test at a constant voltage of 0.7 V at 600 °C.

Acknowledgement

The authors acknowledge gratefully the financial support of the Department of Energy Nuclear Energy University Program (NEUP) (Award Nos. 09-510 and 10-681).

References

[1] D. Brett, A. Atkinson, N. Brandon, S. Skinner, Chem. Soc. Rev. 37 (2008) 1568.
[2] A. Nowick, Y. Du, Solid State Ionics 77 (1995) 137.
[3] K. Kreuer, Solid State Ionics 136–137 (2000) 149.
[4] H. Iwahara, Y. Asakura, K. Katahira, M. Tanaka, Solid State Ionics 168 (2004) 299.
[5] C. Kokkofitis, M. Ouzounidou, A. Skodra, M. Stoukides, Solid State Ionics 178 (2007) 507.
[6] T. Schober, H. Ringel, Ionics 10 (2004) 391.
[7] J. Phair, S. Badwal, Ionics 12 (2006) 103.
[8] F. Lefebvre-Joud, G. Gauthier, J. Mougin, J. Appl. Electrochem. 39 (2009) 535.
[9] H. Iwahara, T. Esaka, H. Uchida, N. Maeda, Solid State Ionics 34 (1981) 359.
[10] H. Uchida, K. Ogaki, H. Iwahara, Proc. Electrochem. Soc. 87 (9) (1987) 172.
[11] M. Oishi, S. Akoshima, K. Yashiro, K. Sato, J. Mizusaki, T. Kawada, Solid State Ionics 180 (2009) 127.
[12] H. Iwahara, Solid State Ionics 86–88 (1996) 9.
[13] K. Kreuer, Annu. Rev. Mater. Res. 33 (2003) 333.
[14] F. Chen, O. Toft Sørensen, G. Meng, D. Peng, J. Eur. Ceram. Soc. 18 (1998) 1389.
[15] R. Peng, Y. Wu, L. Yang, Z. Mao, Solid State Ionics 177 (2006) 389.
[16] Z. Wu, M. Liu, J. Electrochem. Soc. 144 (6) (1997) 2170.
[17] J. Wang, L. Li, B. Campbell, Z. Lv, Y. Ji, Y. Xue, W. Su, Mater. Chem. Phys. 86 (2004) 150.
[18] S. Yamaguchi, N. Yamada, Solid State Ionics 162–163 (2003) 23.

[19] A. Virkar, H. Maiti, J. Power Sources 14 (1985) 295.
[20] K. Künstler, H. Lang, A. Maiwald, G. Tomandle, Solid State Ionics 107 (1998) 221.
[21] N. Zakowsky, S. Williamson, J. Irvine, Solid State Ionics 176 (2005) 3019.
[22] N. Osman, I. Talib, H. Hamid, Ionics 16 (2010) 561.
[23] C. Zuo, S. Zha, M. Liu, M. Hatano, M. Uchiyama, Adv. Mater. 18 (2006) 3318.
[24] Y. Guo, Y. Lin, R. Ran, Z. Shao, J. Power Sources 193 (2009) 400.
[25] L. Bi, S. Zhang, S. Fang, Z. Tao, R. Peng, W. Liu, Electrochem. Commun. 10 (2008) 1598.
[26] K. Xie, R. Yan, X. Liu, J. Alloys Compd. 479 (2009) L40.
[27] K. Xie, R. Yan, X. Xu, X. Liu, G. Meng, Mater. Res. Bull. 44 (2009) 1474.
[28] K. Xie, R. Yan, X. Liu, J. Alloys Compd. 479 (2009) L36.
[29] F. Zhao, Q. Liu, S. Wang, K. Brinkman, F. Chen, Int. J. Hydrogen Energy 35 (2010) 4258.
[30] L. Bi, S. Zhang, L. Zhang, Z. Tao, H. Wang, W. Liu, Int. J. Hydrogen Energy 34 (2009) 2421.
[31] K. Kunstler, H. Lang, A. Maiwald, G. Tomandl, Solid State Ionics 107 (1998) 221.
[32] H. Matsumoto, Y. Kawasaki, N. Ito, M. Enoki, T. Ishihara, Electrochem. Solid-State Lett. 10 (4) (2007) B77.
[33] E. Fabbri, T. Oh, S. Licoccia, E. Traversa, E. Wachsman, J. Electrochem. Soc. 156 (2009) B38.
[34] C. Xia, M. Liu, J. Am. Ceram. Soc. 84 (8) (2001) 1903.
[35] N. Osman, I. Talib, H. Hamid, A. Jani, Ionics 14 (2008) 407.
[36] E. Gorbova, V. Maragou, D. Medvedev, A. Demin, P. Tsiakaras, J. Power Sources 182 (2008) 207.
[37] J. Frade, Solid State Ionics 78 (1995) 87.
[38] T. Suzuki, Z. Hasan, Y. Funahashi, T. Yamaguchi, Y. Fujishiro, M. Awano, Science 325 (5942) (2009) 852.
[39] F. Zhao, F. Chen, Int. J. Hydrogen Energy 35 (2010) 11194.
[40] S. Adler, Chem. Rev. 104 (2004) 4791.
[41] K. Katahira, Y. Kohchi, T. Shimura, H. Iwahara, Solid State Ionics 138 (2000) 91.